Phosphorylation cycling of Annexin A2 Tyr23 is critical for calcium-regulated exocytosis in neuroendocrine cells.

Marion Gabel, F. Delavoie, Cathy Royer, T Tahouly, Stephane Gasman, Marie-France Bader, Nicolas Vitale, Sylvette Chasserot

Phosphorylation cycling of Annexin A2 Tyr23 is critical for calcium-regulated exocytosis in neuroendocrine cells

****

Marion GABEL, Franck DELAVOIE, Cathy ROYER#, Tam TAHOULY, Stéphane GASMAN, Marie-France BADER, Nicolas VITALE and Sylvette CHASSEROT-GOLAZ*

INCI, UPR3212 CNRS, Université de Strasbourg, # Plateforme Imagerie In Vitro, Neuropôle de Strasbourg, *5 rue Blaise Pascal, F-6708, Strasbourg-France.* **** Laboratoire de Biologie Moléculaire Eucaryote,*** *Centre de Biologie Intégrative (CBI), Université de Toulouse, 118 route de Narbonne, F-31000, Toulouse,-France.*

Proofs and correspondence to:

Dr. S.CHASSEROT-GOLAZ (address as above)

Tel.: 33-88-45-67-39

Fax: 33-88-60-16-64

E-mail: chasserot@inci-cnrs.unistra.fr

The abbreviations used are:

AnxA2: Annexin A2
CTx: cholera toxin
DBH: dopamine-beta-hydroxylase
GFP: green fluorescent protein
GST: glutathione S-transferase
PA: phosphatidic acid
PIP_2: phosphatidylinositol 4, 5-bisphosphate
PS: phosphatidylserine
pTyr23AnxA2: Tyr23 phosphorylated form of AnxA2
WT: wild-type

ABSTRACT

Annexin A2 (AnxA2) is a calcium and lipid binding protein involved in neuroendocrine secretion. We have previously demonstrated that AnxA2 participates in the formation and/or stabilisation of lipid microdomains required for structural and spatial organization of the exocytotic machinery in chromaffin cells. However, the regulation of AnxA2 is not fully understood. Numerous phosphorylation sites have been identified in the amino-terminal domain of AnxA2. Phosphorylation of Ser25 and Tyr23 are well established and confirmed to be functionally significant. In particular, phosphorylation of Tyr23 by the tyrosine kinase pp60Src reduces the binding of AnxA2 to both actin filaments and the plasma membrane, two major actors of exocytosis, thus, we examined whether AnxA2 was phosphorylated on Tyr23 during exocytosis. Using immunolabelling and a biochemical approach, we found that nicotine stimulation triggered the phosphorylation of Anx A2 on Tyr23. The expression of two AnxA2 mutants carrying phosphorylation deficient (Y23A) or phosphomimetic (Y23E) mutations reduced the number exocytotic sites. Furthermore, expression of AnxA2-Y23A inhibited the formation of lipid microdomains, whereas the expression of AnxA2-Y23E altered actin filaments associated with docked granules. These results suggest that phosphorylation/dephosphorylation switch at Tyr23 in AnxA2 is critical for calcium-regulated exocytosis in neuroendocrine cells.

KEYWORDS:

Exocytosis - Annexin A2 - Phosphorylation - F-Actin - Lipid domains - Chromaffin cells-

1. INTRODUCTION

Molecules such as neurotransmitters and hormones are secreted by calcium-regulated exocytosis [1, 2]. In neuroendocrine cells, exocytosis implies the recruitment and subsequent fusion of secretory granules at specific sites of the plasma membrane. Annexin A2 (AnxA2) was the first protein identified at these exocytotic sites in chromaffin cells releasing catecholamine [3]. Since then, AnxA2 was shown to bind two major actors of exocytosis, actin and phospholipids. Electron tomography of chromaffin cells revealed that actin filaments bundled by AnxA2 contribute to the formation of GM1-enriched lipid micro-domains required for the spatial organisation of fusion sites at the plasma membrane [4, 5]. Yet, the mechanism(s) regulating AnxA2 activity during exocytosis is an important aspect that remains poorly understood.

The N-terminal domain of AnxA2 has many potential regulatory sites. These include phosphorylation sites at Tyr23 and Ser25 that have been proposed to control the activity and functions of AnxA2. In chromaffin cells, AnxA2-Ser25 phosphorylation by protein kinase C occurs in response to nicotine stimulation and has been linked to granule exocytosis [6-9]. AnxA2 has also been identified as the major substrate for the Src family of tyrosine kinases [10]. Src-dependent phosphorylation of AnxA2-Tyr23 has been reported to modulate actin and membrane binding properties of AnxA2 without affecting the tetramer formation with S100A10 [11-13]. Moreover, AnxA2-Tyr23 phosphorylation induces a conformational change that stabilizes AnxA2 at the membrane and promotes the binding of AnxA2 with phosphatidic acid (PA) (Morel and Gruenberg, 2009), a lipid described as an essential component for exocytosis [14]. Chromaffin cells are enriched in tyrosine kinases such as c-Src [15] and Fyn [16]. Additionnally, nicotine-induced stimulation of chromaffin cells and catecholamine secretion is accompanied by the activation of pp60c-src kinase [17, 18] and rapid tyrosine phosphorylation of multiple cellular proteins [19].

Tyr23 phosphorylation of AnxA2 was first reported to be involved in endocytosis, particularly in the internalisation of the insulin receptor [20]. Phosphorylated Tyr23 seems to be necessary for the stable association of AnxA2 with endosomes, and for their early-stage transport [14]. The role of AnxA2-Tyr23 phosphorylation during regulated secretion has not been studied. Here, using phosphodead and phosphomimetic mutants of AnxA2-Tyr23 generated by site-directed mutagenesis and a combination of immunocytochemical and biochemical approaches, we investigated the functional importance of Tyr23 phosphorylation

during exocytosis in chromaffin cells. Our results suggest a model in which phosphorylation/dephosphorylation of AnxA2-Tyr23 regulates both lipid microdomains formation and actin filament bundling at exocytotic sites, thereby contributing to the fine tuning of regulated exocytosis.

2. MATERIALS & METHODS

2.1 Antibodies and reagents

Rabbit polyclonal antibodies directed against Anx-A2 (p36) purified from bovine aorta were diluted 1:200 (generous gift from J.C. Cavadore, Inserm U-249). Rabbit polyclonal antibodies directed against dopamine ß-hydroxylase (EC.1.14.17.1: DBH) were diluted 1:75 to specifically label exocytotic sites and 1:300 to label secretory granules in chromaffin cells [7]. Monoclonal antibodies anti-pTyr23-AnxA2 (85.Tyr24) and anti-phosphotyrosine (clone 4G10) were purchased by Santa Cruz and Merck-Millipore respectively. Polyclonal antibodies against GFP (IhIP grade) were from Abcam. Secondary coupled to Alexa Fluor® conjugates (488 or 647) or gold particles were from Molecular Probes (Invitrogen, Cergy Pontoise, France) and Aurion (Wageningen, NL) respectively. Fluorescent cholera toxin B subunit coupled to Alexa Fluor® 598, was from Molecular Probes (Thermo Fisher Scientific Inc., Waltham, MA, USA).

2.2 Chromaffin cells

Chromaffin cells were isolated from fresh bovine adrenal glands by retrograde perfusion with collagenase, purified on self-generating Percoll gradients and maintained in culture as previously described [21]. To induce exocytosis, chromaffin cells were washed twice with Locke's solution (140 mM NaCl, 4.7 mM KCl, 2.5 mM $CaCl_2$, 1.2 mM KH_2PO_4, 1.2 mM $MgSO_4$, 11 mM glucose, 0.56 mM ascorbic acid, 0.01 mM EDTA and 15 mM Hepes, pH 7.5), and then stimulated with Locke's solution containing 20 µM nicotine or depolarising solution, K^+ 59mM.

2.3 Quantification of catecholamine secretion

Chromaffin cells maintained in 96-well plates (Thermo Fisher Scientific, France) were briefly washed twice with Locke and processed as stated in the figure legends. Aliquots of the medium were collected at the end of each experiment and cells were lysed with 1% (v/v) Triton X-100 (Sigma, UK). Both sets of samples were assayed fluorimetrically for catecholamine content as previously described [22]. Briefly, 20 µl of sample were transferred to 96-well black-plates (Thermo Fisher Scientific, France), 150 µl of CH_3COONa (1M, pH 6) and 15 µl of $K_3Fe(CN)_6$ (0.25%) were added to each well to oxidize catecholamines to adrenochrome. Next 50 µl of NaOH (5M) containing ascorbic acid (0.3 mg/ml) were added, to

convert adrenochrome to adrenolutin [23]. The fluorescence emitted by adrenolutin (λ_{ex}: 430 nm, λ_{em}: 520 nm) is measured with a spectrofluorometer (LB940 Mithras, Berthold). For each experiment a standard curve was determined using known concentration of adrenaline and noradrenaline to demonstrate that the values obtained were in the linear range of detection of the assay. Amounts released were expressed as a percentage of the total amount of catecholamine present in the cells.

2.4 DNA constructs and cell transfection

Using Quick Change mutagenesis kit (Agilent Technologies, Massy, France), Anx-A2-Y23A-GFP and Anx-A2-Y23E-GFP were generated in human recombinant Anx-A2 fused with GFP [24]. Recombinant GST-Anx-A2 WT GST-Anx-A2-Y23A and GST-Anx-A2-Y23E were produced in E. coli and purified on glutathione-sepharose (GE Healthcare, Upsala, Sweden) as previously described [25]. The purity was estimated at 98% by Coomassie blue staining of SDS-PAGE gels. Plasmids (3 µg) were transfected into chromaffin cells (5 x 10^6 cells) by electroporation (Amaxa Nucleofactor systems, Lonza, Levallois, France) according to the manufacturer's instructions. Electroporated cells were immediately recovered in warm culture medium and plated onto fibronectin-coated glass coverslips. Experiments were performed 48 h after transfection.

2.5 In vitro liposomes binding assays

Liposome preparation was performed as described previously [26]. Lipids solubilized in chloroform were purchased from Avanti Polar Lipids. Liposome mixtures were prepared in mass ratios composed of 85% PC, 5% PE-NBD, and 10% PA, PS, or $PI(4,5)P_2$. Lipids were dried in a stream of nitrogen gas and kept under vacuum for at least 2 h. Dried lipids were then suspended at a concentration of 1.65 mg/ml in liposome-binding buffer (LBB: 20 mM HEPES, pH 7.4, 150 mM NaCl, 1 mM $MgCl_2$) by three freeze and thaw cycles and were extruded using a Mini-Extruder (Avanti) through polycarbonate track-etched membrane filters to produce liposomes usually 200 nm in diameter. The size distribution of liposomes was estimated by dynamic light scattering using a Zetasizer NanoS from Malvern Instruments equipped with a 4-milliwatt laser. Samples were diluted 1:100 in LBB and analyzed at 20°C using 10 runs, each composed of 14 measurements. Quantification of liposome binding to 330 pmol of GST-Anx-A2 WT GST-Anx-A2-Y23A and GST-Anx-A2-Y23E linked to GSH-Sepharose beads was estimated after 20 min incubation in the dark at room temperature and

under agitation with liposomes containing a 10-fold molar excess of PA, PS, or $PI(4,5)P_2$ relative to the quantity of GST proteins in a final volume of 200 µl of LBB. Beads were washed three times with 1 ml of ice-cold LBB and collected by centrifugation at 3000 rpm for 5 min. Liposome binding to beads was estimated by measuring the fluorescence at 535 nm with a Mithras (Berthold) fluorimeter. Triplicate measurements were performed for each condition. Fluorescence measured with GST linked to GSH-Sepharose beads alone was between 3 and 4 A.U. and was subtracted from sample measurements.

2.6 In vitro F-actin binding experiments

The F-actin-bundling activity of recombinant GST-Anx-A2s was tested *in vitro* using the non-muscle actin binding protein Spin-Down Biochem kit (Cat BK013, Cytoskeleton, Denver, CO, USA). Formation of actin bundles was assessed by electron microscopy [27], recombinant AnxA2 proteins were incubated with actin filament during 20 min and an aliquots (5 µl) were spread on electron grids, negatively stained with phosphotungstic acid 1% in water. The samples were observed using a Hitachi 7500 transmission electron microscope.

2.7 Immunofluorescence and confocal microscopy

For immunocytochemistry, chromaffin cells, grown on fibronectin-coated glass coverslips, were fixed and labelled as described previously [7]. GM1 was labelled on live chromaffin cells incubated for 10 min with 8 µg/ml fluorescent cholera toxin B subunit (coupled with Alexa Fluor® 598) in Locke's solution with or without 20 µM nicotine. The transient accessibility of DBH to the plasma membrane of chromaffin cells was tested by incubating cells for 10 min in Locke's solution containing 20µM nicotine and anti-DBH antibodies diluted to 1:75. F-actin was stained with TRITC-conjugated phalloidin (0.5 µg/ml) for 15 min in the dark at room temperature. Labelled cells were visualised using a Leica SP5II confocal microscope. The amount of cholera toxin or DBH labelling associated with the plasma membrane was measured with ICY software and expressed as the average fluorescence intensity normalised to the corresponding surface area, and divided by the total perimeter of each cell. This allowed a quantitative cell-to-cell comparison of the fluorescence detected in cells.

2.8 Plasma membrane sheet preparation and transmission electron microscopy observation

Cytoplasmic face-up membrane sheets were prepared and processed as previously described [28]. Briefly, carbon-coated Formvar films on nickel electron grids were spilled on unstimulated or nicotine-stimulated chromaffin cells. To prepare membrane sheets, a pressure was applied to the grids for 20 s then grids were lifted so that the fragments of the upper cell surface adhered to the grid. These fragments were fixed in 2% paraformaldehyde for 10 min at 4°C immediately after cell stimulation and sheet preparation, which required less than 30 s. After blocking in PBS with 1% BSA and 1% acetylated BSA, the immune labelling was performed and revealed with 25 nm gold particles-conjugated secondary antibodies. These membrane sheets were fixed in 2.5% glutaraldehyde in PBS, postfixed with 0.5% OsO4, dehydrated in a graded ethanol series, treated with hexamethyldisilazane (Sigma-Aldrich, St. Louis, MO, USA), air-dried and observed using a Hitachi 7500 transmission electron microscope.

2.9 Electron tomography and image processing

Tilt series were acquired on a JEOL JEM-2100 transmission electron microscope operated at 200 kV. Data were automatically acquired using Digital Micrograph software. Typically, the tilt ranged between - 60 and + 60 with 2° angular increments. Images were recorded at a nominal magnification of 5,000 X or 10,000 X on a Gatan Ultrascan 2K×2K CCD camera with a defocus range of −4 µm to -8 µm. Alignments and weighted back-projection-based reconstructions of raw tilt series, using patch tracking algorithm, were computed with IMOD software package [29]. Three-dimensional reconstructions were visualised with UCSF Chimera [30] using the surface or solid rendering mode.

2.10 Statistical analysis

As specified in figure legends, group of data are presented as mean (± SEM) or median and were analysed using a Mann-Whitney test. Asterisks in each box and whisker plot indicate statistical significance (*= $P < 0.05$; **= $P < 0.01$; ***= $P < 0.001$).

3. RESULTS

3.1 AnxA2 is phosphorylated on Tyr23 at an early stage of exocytosis

To determine whether AnxA2 is tyrosine phosphorylated during exocytosis, double-labeling experiments to visualize tyrosine phosphorylated proteins and AnxA2 were performed. We have previously shown that AnxA2 translocates to the periphery of 80% of chromaffin cells after 3 minutes of stimulation with nicotine [31]. Thus in this condition, we found that nicotinic stimulation of chromaffin cells triggered the translocation of AnxA2 at the plasma membrane together with a significant increase of tyrosine phosphorylated proteins at the cell periphery (Figure 1A), in agreement with a previous report [19]. The co-localization of AnxA2 with tyrosine-phosphorylated protein labeling in the cell periphery (Figure 1A) suggested that AnxA2 might be phosphorylated in the subplasmalemal area of stimulated cells. To test this hypothesis, western-blot analyses were performed using an antibody specifically directed against pTyr23AnxA2 (Figure 1B). Densitometric scanning revealed that the ratio of pTyr23AnxA2/total AnxA2 increased by 5 in stimulated cells, indicating that AnxA2 is phosphorylated on Tyr23 during exocytosis. As shown in Figures 1C and D, Tyr23 phosphorylation preceded the peak of chromogranin A and catecholamine secretion, being maximal after 30 seconds of stimulation. It is interesting to note that AnxA2 was much less phosphorylated at maximal secretion, suggesting that dephosphorylation already starts during the exocytotic process. Altogether, these data demonstrate that a dynamic tyrosine phosphorylation/dephosphorylation cycle of AnxA2 occurs during exocytosis.

3.2 Tyr23 phosphorylation of AnxA2 increases in vitro binding to phosphatidylserine (PS) and phosphatidic acid (PA) but decreases in vitro actin bundling activity.

To study the functional importance of AnxA2 phosphorylation on Tyr23, two AnxA2 mutants were generated by site-directed mutagenesis: a phosphodead mutant in which Tyr23 is replaced by an alanine (AnxA2-Y23A) and a phosphomimetic mutant in which Tyr23 is replaced by glutamic acid (AnxA2-Y23E). AnxA2-Wild Type (AnxA2-WT) and the mutants were expressed as recombinant proteins fused to glutathione S-transferase (GST) for *in vitro* experiments. Since Tyr23 phosphorylation might affect lipid interaction, we examined the

binding of AnxA2-WT and mutated AnxA2 to different phospholipids potentially present at the exocytotic sites [32, 33]. Binding assays were performed with glutathione S-transferase (GST)-fused recombinant AnxA2 proteins incubated with fluorescent liposomes enriched in PIP_2, PS or PA, in presence or absence of calcium [26]. In line with a previous report [12], AnxA2-WT was found to bind more efficiently to negative phospholipids in the presence of calcium (Figure 2A). Binding of AnxA2 to PIP_2 was not significantly modified by the mutations (Figure 2A). In contrast, binding of the phosphomimetic AnxA2-Y23E mutant to PA or PS was enhanced by 2.5 fold compared to AnxA2-WT or to AnxA2-Y23A. This observation is in agreement with previous results showing that AnxA2-Y23E interacts more efficiently than AnxA2-Y23A with liposomes containing PA [14]. This suggests that AnxA2 phosphorylation on Tyr23 does not seem to affect PIP_2 binding but increased binding to other negatively charged phospholipids such as PA and PS.

Next, the *in vitro* actin binding and aggregating activities of AnxA2-WT and AnxA2 mutants were compared using GST-coupled recombinant proteins incubated with F-actin in the absence or presence of calcium [34]. GST-AnxA2-WT, GST-AnxA2-Y23A and GST-AnxA2-Y23E were able to bind and aggregate F-actin in a calcium-dependent manner (data not shown). Figure 2B illustrates the ultrastructure of the F-actin/Anx-A2 aggregates examined by electron microscopy. GST-AnxA2-WT and GST-AnxA2-Y23A formed actin bundles with linearly ordered filaments. In contrast, GST-AnxA2-Y23E was unable to bundle polymerized actin, which appeared as disordered filaments. To summarize these *in vitro* observations, the phosphomimetic mutation Y23E enhances the binding of monomeric AnxA2 to PS and PA but prevent its capacity to form actin bundles.

3.3 The phosphorylation of Tyr23 is necessary for the formation of lipid microdomains formed at the plasma membrane of chromaffin cells undergoing exocytosis

To examine whether Tyr23 phosphorylation may interfere with the AnxA2-mediated lipid micro-domains formed at the exocytotic sites in stimulated cells [31], AnxA2-WT and AnxA2 mutants were expressed in chromaffin cells as C-terminal GFP fusion proteins [35, 36] and cells were stimulated in the presence of fluorescent cholera toxin to visualize the formation of GM1 domains [31]. As illustrated in Figure 3A, cell stimulation triggered equally well the translocation of the three forms of AnxA2 to the cell periphery. Cholera toxin

labeling was similar in cells expressing AnxA2-WT or AnxA2-Y23E mutant than in non-transfected cell (control). In contrast, cholera toxin labeling decreased in cells expressing the phosphodead AnxA2-Y23A mutant. Semi-quantitative analysis confirmed that expression of the mutant Y23A reduced GM1 labeling suggesting a defect in lipid micro-domains formation (Figures 3A and B). Altogether these observations suggest that Tyr23 phosphorylation of AnxA2 is implicated in the formation of lipid micro-domains at the plasma membrane of secretagogue-activated chromaffin cells.

3.4 Tyr23 phosphorylation of AnxA2 plays a role in exocytosis

To investigate the impact of AnxA2 Tyr23 phosphorylation on secretion, chromaffin cells expressing AnxA2-WT and AnxA2 mutants were stimulated in the presence in the extra-cellular medium of an antibody directed against dopamine-beta-hydroxylase (DBH) [31]. As DBH is a luminal secretory granule marker, it becomes accessible to the extracellular anti-DBH antibodies only after full fusion of secretory granules with the plasma membrane, thereby revealing the sites of exocytosis. Figures 4A and B show that expression of phosphodead AnxA2-Y23A and phosphomimetic AnxA2-Y23E decreased cell surface DBH labeling compared to AnxA2-WT or to non-transfected cells by approximately 60%, indicating a significant reduction of exocytotic activity in stimulated cells expressing AnxA2 mutants. These effects are not likely the consequence of a decrease of DBH level in these cells because DBH labelling in permeabilized chromaffin cells expressing the different AnxA2 constructions were not significantly affected (Figure 4C). These results support the idea that the phosphorylation status of the AnxA2 Tyr23 residue is of functional significance for neuroendocrine secretion. The inhibition of secretion observed in cells expressing the phosphodead AnxA2 mutant is in line with the inhibition of lipid domain formation induced by this mutant (Figure 3). The inhibition of secretion observed in cells expressing the phosphomimetic mutant of AnxA2 could be a consequence of its decreased actin bundling activity (Figure 2B).

3.5 Tyr23 phosphorylation of AnxA2 affects the recruitment of secretory granules to the plasma membrane

To determine more precisely which stage of exocytosis is controlled by Tyr23 phosphorylation, we prepared plasma membrane sheets from cells expressing the two AnxA2 mutants and counted the number of docked granules. Membrane sheets of transfected cells were identified using an anti-GFP antibody visualized by 25 nm beads [34]. As illustrated Figure 5, the number of docked granules is largely decreased in cells expressing the AnxA2-Y23A mutant compared to non-transfected cells (control) or cells expressing AnxA2-WT. Expression of the phosphomimetic mutant also decreased the amount of docked secretory granule although to a smaller extent. These results together with the decrease of exocytotic activity revealed by DBH labelling (Figure 4) suggest that the phosphorylation status of AnxA2 Tyr23 plays a role in exocytosis by controlling secretory granule docking at the plasma membrane.

At higher magnification, docked granules appeared somewhat different in cells expressing the two AnxA2 mutants (Figure 5C). In cells expressing AnxA2-Y23A, granules were smooth devoid of actin filaments. In cells expressing AnxA2-Y23E, granules displayed actin filaments connecting them to plasma membrane but filaments were much thinner than in cells expressing AnxA2-WT (Figure 5C), in agreement with the *in vitro* observations indicating that GST-AnxA2-Y23E was unable to form bundles of actin filaments (Figure 3). To probe this model, electron tomography was performed on plasma membrane sheets obtained from cells expressing the phosphomimetic mutant AnxA2-Y23E. After 3D reconstruction, defects in the actin bundles connecting secretory granules to the plasma membrane clearly appeared in stimulated cells expressing AnxA2-Y23E (Figure 6B) compared to AnxA2-WT cells (Figure 6A). In the phosphomimetic mutant expressing cells, secretory granules appeared linked to the plasma membrane by a thin structure, most likely a thin actin microfilament (Figure 6D) whereas in the AnxA2-WT cells, F-actin connecting granules to the plasma membrane was organized into a complex network of bundles and branches (Figure 6C). These results are consistent with the hypothesis that the phosporylation-dephosphorylation cycle of AnxA2 has a key role in the cortical actin rearrangement occurring at the stage of granule docking during exocytosis.

3 DISCUSSION

During neuroendocrine secretion, AnxA2 has been shown to participate together with the actin cytoskeleton in the formation of lipid microdomains required for docking and fusion of secretory granules with the plasma membrane. [28, 31, 34]. The N-terminal domain of AnxA2 contains many phosphorylation sites that modulate the three-dimensional structure of the protein and regulate its affinity for different partners [12, 13, 37]. In particular, phosphorylation of Tyr23 has been described to modify AnxA2 binding to membranes and actin [38], two major players of the exocytotic machinery [31, 34]. Yet, until recently the importance of AnxA2-Tyr23 phosphorylation in the context of exocytosis has never been studied. The present report describes that AnxA2 is phosphorylated on Tyr23 during an early step of the secretory process and provides further evidence that this phosphorylation step is critical for exocytosis. Expression of AnxA2-Tyr23 phosphomimetic and phosphodead mutants in chromaffin cell indicate that a Tyr23 phosphorylation/dephosphorylation cycle is required for both the formation of lipid domains and the docking of secretory granules to the plasma membrane. We propose that AnxA2-Tyr23 is first phosphorylated to promote lipid domain formation required for secretory granule recruitment and subsequently dephosphorylated to facilitate the formation of actin bundles that stably anchor secretory granules to the plasma membrane. On the other hand, phosphorylation/dephosphorylation cycle of the AnxA2-Ser-25 has also been involved in chromaffin cells secretion [8] and phosphorylation of AnxA2-Ser11 by PKC induces the dissociation of AnxA2 tetramer [4]. In the light of these previous studies and on our results concerning the role of phosphorylation/dephosphorylation cycle of Tyr23 during exocytosis, we propose the following sequence of events depicted in Figure 7. Upon cell stimulation, AnxA2 translocates to the plasma membrane and is phosphorylated on Tyr23 to organize lipid microdomains required for the sites of exocytosis. Tyr23 is then dephosphorylated to activate the actin bundling activity and form an actin network that stably anchors docked granules and Ser25 is phosphorylated by PKC for the late fusion step. Finally, phosphorylation on Ser11 triggers the dissociation of the AnxA2 tetramer, the relocation of AnxA2 monomer into the cytoplasm and ends the exocytotic process. Thus, the fine-tuning of AnxA2 functions in the exocytotic machinery is likely to be mediated by the coordinated modification of its three main phosphorylation sites.

4.1 Phosphorylation of AnxA2-Tyr23 is necessary for the formation of exocytotic sites

We show here that phosphorylation of AnxA2-Tyr23 is an early event after stimulation, preceding the bulk of chromogranin A and catecholamine secretion. In line, we previously described in chromaffin cells that nicotine triggers within seconds the rapid incorporation of ^{32}P into AnxA2 [7]. This incorporation of ^{32}P was primarily observed in Anx2 associated to a detergent-insoluble fraction, an observation suggesting that the translocation of AnxA2 to the cell periphery may precede the phosphorylation process [7]. Indeed, Tyr23 becomes more exposed and accessible when AnxA2 is associated with the plasma membrane [39] and phosphorylation induces a conformational change that stabilizes AnxA2 at the membrane [14], further supporting the idea that AnxA2 is phosphorylated just after translocation to the membrane. The fact that the AnxA2-Y23E mutant has a higher affinity for PA and PS than AnxA2-WT, and conversely that the mutant AnxA2-Y23A inhibits the formation of lipid microdomains, led us to conclude that AnxA2 must be phosphorylated to form lipid domains. It is likely that the increased affinity of pTyr23AnxA2 for PA and PS might recruit and locally increase the concentration of these lipids and thus favor the formation of lipid microdomains.

In cells expressing the phosphodead mutant AnxA2-Y23A, analysis of membrane sheets by electron microscopy revealed that the number of granules docked at the plasma membrane was greatly reduced. Docking inhibition might be a direct consequence of the inhibition of lipid platform formation where specific proteins required for efficient docking are concentrated. It is noteworthy that in cells expressing the AnxA2-Y23A mutant, secretory granules docked at the plasma membrane appeared smoother, presumably reflecting the absence of an actin coat [34]. Thus, disorganization of the lipid platform due to the absence of AnxA2-Tyr23 phosphorylation results also in a defect of the actin cytoskeleton surrounding granules. A possible explanation is that inhibition or destabilization of lipid micro-domains in the absence of Tyr23 phosphorylation affects also the recruitment of proteins, such as the Rho GTPases, involved in the synthesis of actin filaments and granule coat formation in the late stages of exocytosis [40].

4.2. AnxA2-Tyr23 needs to be dephosphorylated in the final stages of exocytosis

In cells expressing AnxA2-Y23E mutant, lipid microdomain formation was apparently not impaired but yet exocytosis was strongly inhibited and less secretory granules were found docked to the plasma membrane. These findings suggest that an AnxA2-Tyr23 dephosphorylation step might be needed to further proceed for exocytosis. Phosphorylation of AnxA2-Tyr23 and Ser25 are mutually exclusive [37]. Thus, a first explanation might be that Tyr23 needs to be dephosphorylated to allow the phosphorylation of Ser25 required for the late fusion step of exocytosis [8]. Alternatively, we show here that the AnxA2-Y23E mutant is unable to bundle actin filaments *in vitro*. Moreover, in stimulated cells expressing the phosphomimetic AnxA2-Y23E mutant, the actin network wrapping docked secretory granule and possibly connecting them to the plasma membrane appeared reduced in size and organization. Thus, an interesting possibility is that dephosphorylation of Tyr23 might be needed to relieve the actin bundling activity of AnxA2. Thereafter, the AnxA2-mediated actin network might be required to stabilize granules docked to the plasma membrane by a minimal tethering machinery and/or to squeeze granules for effective content release after fusion [34, 41].

4.3 Regulation of the AnxA2-Tyr23 phosphorylation/dephosphorylation cycle in the course of exocytosis

The nature of the kinase and phosphatase involved in this phosphorylation/dephosphorylation cycle of the AnxA2-Tyr23 remains to be identified. AnxA2 is the major substrate of the pp60Src kinase in bovine intestinal epithelial cells [42]. Other Src family kinases, such as Lyn tyrosine kinase are associated with lipid domains [43] and Fyn tyrosine kinase is calcium sensitive and associated with chromaffin cell membranes [44]. Thus, at first view, the Src kinase family members represent potential candidates. However, Tyr23 phosphorylation of AnxA2 is an early event of exocytosis, whereas Src kinases have been involved in late stages of exocytosis such as the fusion pore expansion [18]. Moreover, the Src family tyrosine kinase inhibitor PP2 did not inhibit phosphorylation of AnxA2-Tyr23 in chromaffin cells (data not shown) questioning the role of the Src family kinases in the Tyr23 phosphorylation of AnxA2 during secretion. Another interesting candidate would be the tyrosine kinase Erythropoietin-producing human hepatocellular

receptor (EPH) B6 (EPHB6) recently described to regulate catecholamine release in chromaffin cells [45] but this remains to be investigated.

An inportant observation is that AnxA2 must be dephosphorylated after formation of lipid domains. Thus, it would also be interesting to identify the phosphatase involved. In chromaffin cells, molecular complexes displaying both tyrosine kinase and tyrosine phosphatase activity have been described at the plasma membrane [46]. In addition, some phosphatases are preferentially localized in lipid domains [47], and thus could dephosphorylate AnxA2 at this stage. The calcium-sensitive phosphatase Src homology 2 (SH2)-containing protein tyrosine phosphatase (Shp2) is an interesting candidate because Shp2 can interact with AnxA2 in the presence of cholesterol [48, 49], Shp2 is highly specific for phosphorylated AnxA2-Tyr23 [50] and Shp2 is expressed in chromaffin cells.

4 CONCLUSION

The multifunctionality of AnxA2 in chromaffin cells is subjected to a particularly complex regulation via ligand binding such as S100A10, subcellular targeting (cytosol versus plasma membrane) and post-translational modifications i.e. phosphorylation and dephosphorylation on tyrosine and serine residues. We show here that two essential functions of AnxA2 during regulated exocytosis i.e. the regulation of lipid micro-domain formation and cytoskeleton organization may be under the control of the phosphorylation/dephosphorylation cycle of Tyr23.

ACKNOWLEDGEMENTS

We are grateful to V. Gerke for generous gift of AnxA2-GFP. We thank the municipal slaughterhouse of Haguenau (France) to provide bovine adrenal glands. We acknowledge N. Grant for helpful comments and critical reading of the manuscript, B Lorber for dynamic light scattering to control liposome size. This work was supported by CNRS, Université de Strasbourg, Inserm and by a grant from Fondation pour la Recherche Médicale to N.V.

BIBLIOGRAPHY

[1] E. Tanguy, O. Carmon, Q. Wang, L. Jeandel, S. Chasserot-Golaz, M. Montero-Hadjadje, N. Vitale, Lipids implicated in the journey of a secretory granule: from biogenesis to fusion, J Neurochem, 137 (2016) 904-912.
[2] J.P. Bombardier, M. Munson, Three steps forward, two steps back: mechanistic insights into the assembly and disassembly of the SNARE complex, Curr Opin Chem Biol, 29 (2015) 66-71.
[3] T. Nakata, K. Sobue, N. Hirokawa, Conformational change and localization of calpactin I complex involved in exocytosis as revealed by quick-freeze, deep-etch electron microscopy and immunocytochemistry, J Cell Biol, 110 (1990) 13-25.
[4] A. Bharadwaj, M. Bydoun, R. Holloway, D. Waisman, Annexin A2 heterotetramer: structure and function, Int J Mol Sci, 14 (2013) 6259-6305.
[5] M. Gabel, S. Chasserot-Golaz, Annexin A2, an essential partner of the exocytotic process in chromaffin cells, J Neurochem, 137 (2016) 890-896.
[6] K.L. Gould, J.R. Woodgett, C.M. Isacke, T. Hunter, The protein-tyrosine kinase substrate p36 is also a substrate for protein kinase C in vitro and in vivo, Mol Cell Biol, 6 (1986) 2738-2744.
[7] S. Chasserot-Golaz, N. Vitale, I. Sagot, B. Delouche, S. Dirrig, L.A. Pradel, J.P. Henry, D. Aunis, M.F. Bader, Annexin II in exocytosis: catecholamine secretion requires the translocation of p36 to the subplasmalemmal region in chromaffin cells, J Cell Biol, 133 (1996) 1217-1236.
[8] B. Delouche, L.A. Pradel, J.P. Henry, Phosphorylation by protein kinase C of annexin 2 in chromaffin cells stimulated by nicotine, J Neurochem, 68 (1997) 1720-1727.
[9] F. Regnouf, I. Sagot, B. Delouche, G. Devilliers, J. Cartaud, J.P. Henry, L.A. Pradel, "In vitro" phosphorylation of annexin 2 heterotetramer by protein kinase C. Comparative properties of the unphosphorylated and phosphorylated annexin 2 on the aggregation and fusion of chromaffin granule membranes, J Biol Chem, 270 (1995) 27143-27150.
[10] E. Erikson, H.G. Tomasiewicz, R.L. Erikson, Biochemical characterization of a 34-kilodalton normal cellular substrate of pp60v-src and an associated 6-kilodalton protein, Mol Cell Biol, 4 (1984) 77-85.
[11] J.R. Glenney, Jr., B. Tack, M.A. Powell, Calpactins: two distinct Ca++-regulated phospholipid- and actin-binding proteins isolated from lung and placenta, J Cell Biol, 104 (1987) 503-511.
[12] V. Gerke, C.E. Creutz, S.E. Moss, Annexins: linking Ca2+ signalling to membrane dynamics, Nat Rev Mol Cell Biol, 6 (2005) 449-461.
[13] A.K. Grindheim, J. Saraste, A. Vedeler, Protein phosphorylation and its role in the regulation of Annexin A2 function, Biochim Biophys Acta, 1861 (2017) 2515-2529.
[14] E. Morel, J. Gruenberg, Annexin A2 binding to endosomes and functions in endosomal transport are regulated by tyrosine 23 phosphorylation, J Biol Chem, 284 (2009) 1604-1611.
[15] S.J. Parsons, C.E. Creutz, p60c-src activity detected in the chromaffin granule membrane, Biochem Biophys Res Commun, 134 (1986) 736-742.
[16] C.M. Allen, C.M. Ely, M.A. Juaneza, S.J. Parsons, Activation of Fyn tyrosine kinase upon secretagogue stimulation of bovine chromaffin cells, J Neurosci Res, 44 (1996) 421-429.
[17] K.M. Oddie, J.S. Litz, J.C. Balserak, D.M. Payne, C.E. Creutz, S.J. Parsons, Modulation of pp60c-src tyrosine kinase activity during secretion in stimulated bovine adrenal chromaffin cells, J Neurosci Res, 24 (1989) 38-48.
[18] M.J. Olivares, A.M. Gonzalez-Jamett, M.J. Guerra, X. Baez-Matus, V. Haro-Acuna, N. Martinez-Quiles, A.M. Cardenas, Src kinases regulate de novo actin polymerization during exocytosis in neuroendocrine chromaffin cells, PLoS One, 9 (2014) e99001.

[19] M.E. Cox, C.M. Ely, A.D. Catling, M.J. Weber, S.J. Parsons, Tyrosine kinases are required for catecholamine secretion and mitogen-activated protein kinase activation in bovine adrenal chromaffin cells, J Neurochem, 66 (1996) 1103-1112.
[20] Y. Biener, R. Feinstein, M. Mayak, Y. Kaburagi, T. Kadowaki, Y. Zick, Annexin II is a novel player in insulin signal transduction. Possible association between annexin II phosphorylation and insulin receptor internalization, J Biol Chem, 271 (1996) 29489-29496.
[21] M.F. Bader, D. Thierse, D. Aunis, G. Ahnert-Hilger, M. Gratzl, Characterization of hormone and protein release from alpha-toxin-permeabilized chromaffin cells in primary culture, J Biol Chem, 261 (1986) 5777-5783.
[22] F.A. Meunier, Z.P. Feng, J. Molgo, G.W. Zamponi, G. Schiavo, Glycerotoxin from Glycera convoluta stimulates neurosecretion by up-regulating N-type Ca2+ channel activity, EMBO J, 21 (2002) 6733-6743.
[23] R.A. Heacock, B.D. Laidlaw, Reduction of adrenochrome with ascorbic acid, Nature, 182 (1958) 526-527.
[24] U. Rescher, D. Ruhe, C. Ludwig, N. Zobiack, V. Gerke, Annexin 2 is a phosphatidylinositol (4,5)-bisphosphate binding protein recruited to actin assembly sites at cellular membranes, J Cell Sci, 117 (2004) 3473-3480.
[25] N. Vitale, J. Moss, M. Vaughan, ARD1, a 64-kDa bifunctional protein containing an 18-kDa GTP-binding ADP-ribosylation factor domain and a 46-kDa GTPase-activating domain, Proc Natl Acad Sci U S A, 93 (1996) 1941-1944.
[26] N. Kassas, E. Tanguy, T. Thahouly, L. Fouillen, D. Heintz, S. Chasserot-Golaz, M.F. Bader, N.J. Grant, N. Vitale, Comparative Characterization of Phosphatidic Acid Sensors and Their Localization during Frustrated Phagocytosis, J Biol Chem, 292 (2017) 4266-4279.
[27] N.W. Ikebuchi, D.M. Waisman, Calcium-dependent regulation of actin filament bundling by lipocortin-85, J Biol Chem, 265 (1990) 3392-3400.
[28] E. Umbrecht-Jenck, V. Demais, V. Calco, Y. Bailly, M.F. Bader, S. Chasserot-Golaz, S100A10-mediated translocation of annexin-A2 to SNARE proteins in adrenergic chromaffin cells undergoing exocytosis, Traffic, 11 (2010) 958-971.
[29] J.R. Kremer, D.N. Mastronarde, J.R. McIntosh, Computer visualization of three-dimensional image data using IMOD, J Struct Biol, 116 (1996) 71-76.
[30] E.F. Pettersen, T.D. Goddard, C.C. Huang, G.S. Couch, D.M. Greenblatt, E.C. Meng, T.E. Ferrin, UCSF Chimera--a visualization system for exploratory research and analysis, J Comput Chem, 25 (2004) 1605-1612.
[31] S. Chasserot-Golaz, N. Vitale, E. Umbrecht-Jenck, D. Knight, V. Gerke, M.F. Bader, Annexin 2 promotes the formation of lipid microdomains required for calcium-regulated exocytosis of dense-core vesicles, Mol Biol Cell, 16 (2005) 1108-1119.
[32] M.R. Ammar, N. Kassas, S. Chasserot-Golaz, M.F. Bader, N. Vitale, Lipids in Regulated Exocytosis: What are They Doing?, Front Endocrinol (Lausanne), 4 (2013) 125.
[33] S. Chasserot-Golaz, J.R. Coorssen, F.A. Meunier, N. Vitale, Lipid dynamics in exocytosis, Cell Mol Neurobiol, 30 (2010) 1335-1342.
[34] M. Gabel, F. Delavoie, V. Demais, C. Royer, Y. Bailly, N. Vitale, M.F. Bader, S. Chasserot-Golaz, Annexin A2-dependent actin bundling promotes secretory granule docking to the plasma membrane and exocytosis, J Cell Biol, 210 (2015) 785-800.
[35] N. Zobiack, V. Gerke, U. Rescher, Complex formation and submembranous localization of annexin 2 and S100A10 in live HepG2 cells, FEBS Lett, 500 (2001) 137-140.
[36] U. Rescher, C. Ludwig, V. Konietzko, A. Kharitonenkov, V. Gerke, Tyrosine phosphorylation of annexin A2 regulates Rho-mediated actin rearrangement and cell adhesion, J Cell Sci, 121 (2008) 2177-2185.
[37] P. Ecsedi, B. Kiss, G. Gogl, L. Radnai, L. Buday, K. Koprivanacz, K. Liliom, I. Leveles, B. Vertessy, N. Jeszenoi, C. Hetenyi, G. Schlosser, G. Katona, L. Nyitray, Regulation of the

Equilibrium between Closed and Open Conformations of Annexin A2 by N-Terminal Phosphorylation and S100A4-Binding, Structure, 25 (2017) 1195-1207 e1195.
[38] I. Hubaishy, P.G. Jones, J. Bjorge, C. Bellagamba, S. Fitzpatrick, D.J. Fujita, D.M. Waisman, Modulation of annexin II tetramer by tyrosine phosphorylation, Biochemistry, 34 (1995) 14527-14534.
[39] C. Bellagamba, I. Hubaishy, J.D. Bjorge, S.L. Fitzpatrick, D.J. Fujita, D.M. Waisman, Tyrosine phosphorylation of annexin II tetramer is stimulated by membrane binding, J Biol Chem, 272 (1997) 3195-3199.
[40] S. Gasman, S. Chasserot-Golaz, M.R. Popoff, D. Aunis, M.F. Bader, Involvement of Rho GTPases in calcium-regulated exocytosis from adrenal chromaffin cells, J Cell Sci, 112 (Pt 24) (1999) 4763-4771.
[41] R.F. Toonen, O. Kochubey, H. de Wit, A. Gulyas-Kovacs, B. Konijnenburg, J.B. Sorensen, J. Klingauf, M. Verhage, Dissecting docking and tethering of secretory vesicles at the target membrane, EMBO J, 25 (2006) 3725-3737.
[42] J.R. Glenney, Jr., B.F. Tack, Amino-terminal sequence of p36 and associated p10: identification of the site of tyrosine phosphorylation and homology with S-100, Proc Natl Acad Sci U S A, 82 (1985) 7884-7888.
[43] D. Matsuda, Y. Nakayama, S. Horimoto, T. Kuga, K. Ikeda, K. Kasahara, N. Yamaguchi, Involvement of Golgi-associated Lyn tyrosine kinase in the translocation of annexin II to the endoplasmic reticulum under oxidative stress, Exp Cell Res, 312 (2006) 1205-1217.
[44] J.A. Spijkers-Hagelstein, S. Mimoso Pinhancos, P. Schneider, R. Pieters, R.W. Stam, Src kinase-induced phosphorylation of annexin A2 mediates glucocorticoid resistance in MLL-rearranged infant acute lymphoblastic leukemia, Leukemia, 27 (2013) 1063-1071.
[45] Y. Wang, W. Shi, A. Blanchette, J. Peng, S. Qi, H. Luo, J. Ledoux, J. Wu, EPHB6 and testosterone in concert regulate epinephrine release by adrenal gland chromaffin cells, Sci Rep, 8 (2018) 842.
[46] M.L. van Hoek, C.S. Allen, S.J. Parsons, Phosphotyrosine phosphatase activity associated with c-Src in large multimeric complexes isolated from adrenal medullary chromaffin cells, Biochem J, 326 (Pt 1) (1997) 271-277.
[47] K. Simons, D. Toomre, Lipid rafts and signal transduction, Nat Rev Mol Cell Biol, 1 (2000) 31-39.
[48] J.C. Yoo, M.J. Hayman, Annexin II binds to SHP2 and this interaction is regulated by HSP70 levels, Biochem Biophys Res Commun, 356 (2007) 906-911.
[49] A. Burkart, B. Samii, S. Corvera, H.S. Shpetner, Regulation of the SHP-2 tyrosine phosphatase by a novel cholesterol- and cell confluence-dependent mechanism, J Biol Chem, 278 (2003) 18360-18367.
[50] X. Wang, R. Yan, J. Song, DephosSite: a machine learning approach for discovering phosphotase-specific dephosphorylation sites, Sci Rep, 6 (2016) 23510.

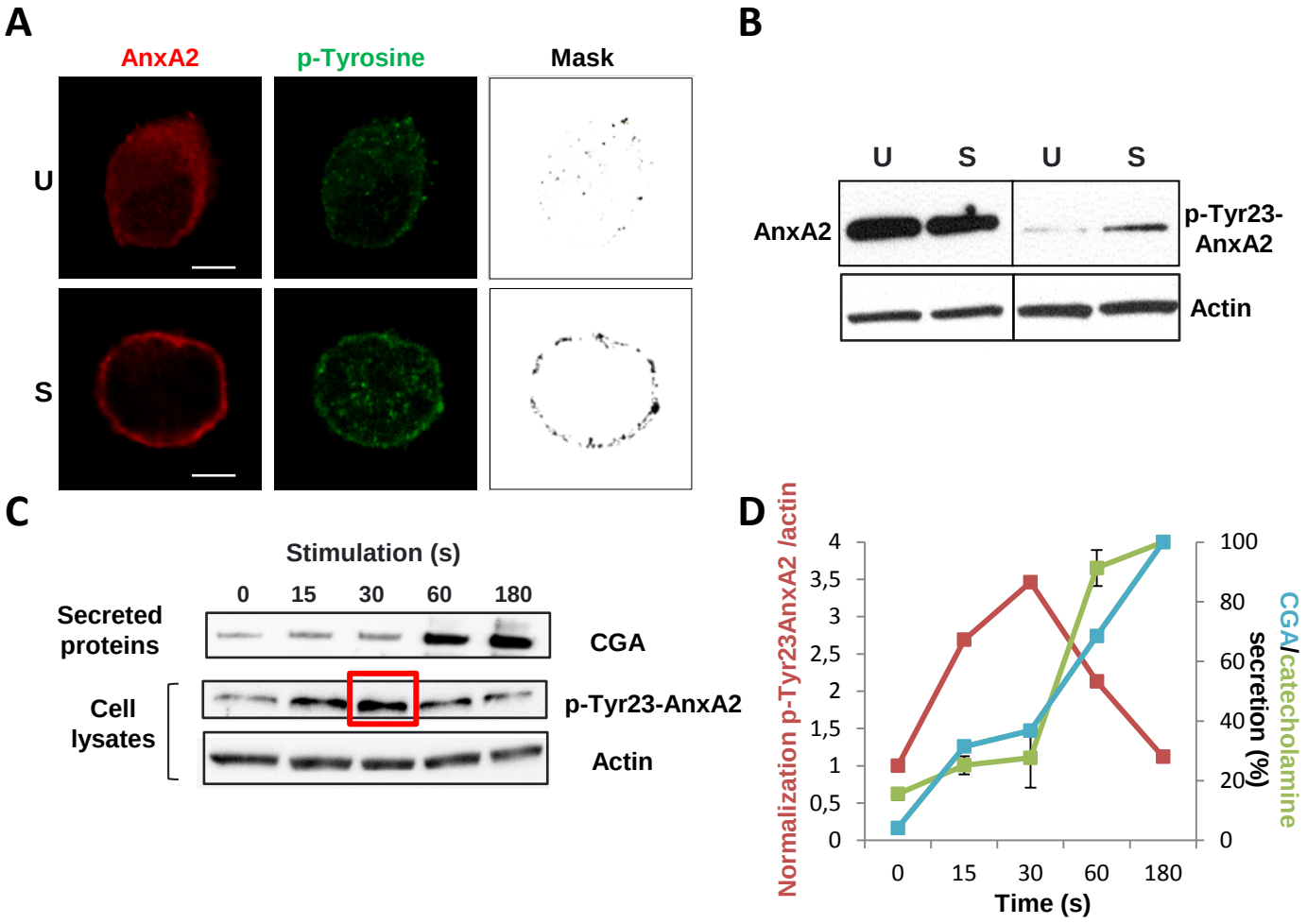

Figure 1: AnxA2 is phosphorylated on Tyr23 during exocytosis

A. Unstimulated (U) or 20 µM nicotine stimulated (S) chromaffin cells were labelled with anti-AnxA2 and anti-P-Tyrosine antibodies and revealed with Alexa Fluor®488-conjugated anti-rabbit and Alexa Fluor®555-conjugated anti-mouse antibodies, respectively. Images were recorded in the same optical section by a dual exposure procedure. Masks representing the region of co-localization were generated by selecting the double-labelled pixels. Bars = 5µm.

B. Lysates obtained from unstimulated (U) or nicotine (20µM)-stimulated (S) chromaffin cells were analyzed by western blot and revealed with anti-actin, anti-AnxA2 and anti-pTyr23-AnxA2 antibodies. Data correspond to a typical experiment representative of 3 independent experiments.

C. Kinetics of AnxA2-Tyr23 phosphorylation in response to cell stimulation. Chromaffin cells were stimulated with 20 µM nicotine for the indicated periods of time. Secreted products were collected and cells lysed. Lysates and secreted proteins were analyzed by western blot on a 12% polyacrylamide gel and revealed with anti-chromogranin A (CGA, secreted proteins) or anti-actin and anti-pTyr23-AnxA2 antibodies (lysates). Data correspond to a typical experiment representative of 3 experiments.

D. Time course of AnxA2 phosphorylation, chromogranin A and catecholamine secretion in nicotine-stimulated chromaffin cells. Data correspond to the same experiment presented pannel C, and are representative of 3 independent experiments.

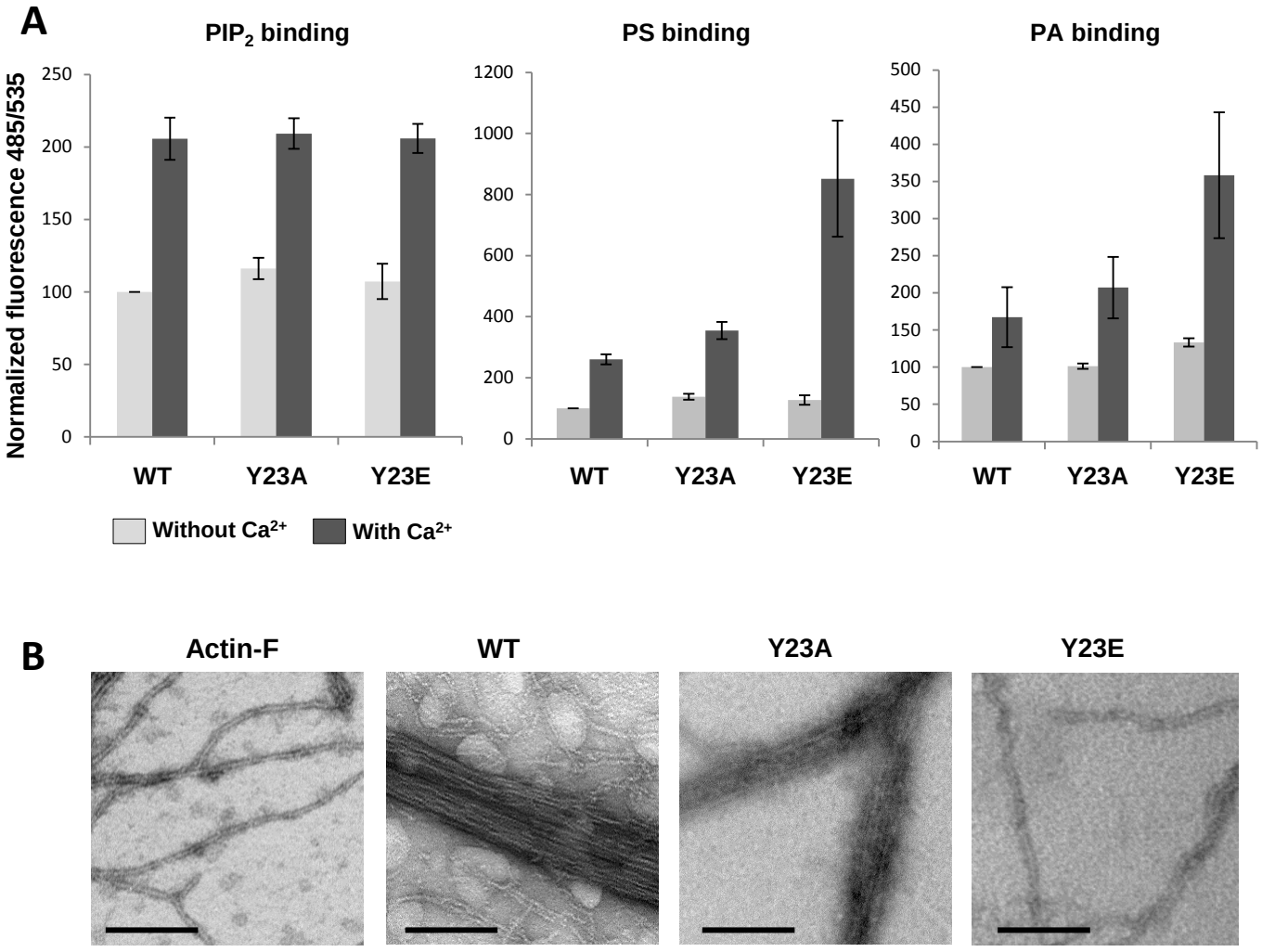

Figure 2: Characterization of AnxA2 mutants

A. Semi-quantitative fluorescent liposome assays performed with GST-AnxA2-beads and liposomes (5% PE-NBD, 85% DOPC, and 10% PIP_2 or PS or PA). Binding of liposomes to GST-AnxA2 beads was estimated by measuring the total fluorescence and subtracting the background (see under "Materials and Methods"). Fluorescence measured when liposomes were incubated with GST alone was around 3 A.U. and was subtracted. Results are presented as means ± S.D. Triplicate measurements pooled from a typical experiment representative of 5 experiments.

B. Electron micrographs showing recombinant Anx-A2/F-actin aggregates. Purified recombinant Anx-A2 proteins fused with GST (4µM) were incubated with pre-formed actin filaments (18µM) for 30 min at room temperature. An aliquot (5µl) was spread on electron grids and prepared for electron microscopy. Data are representative of 2 samples analysed in 3 independent experiments. Bars = 50nm.

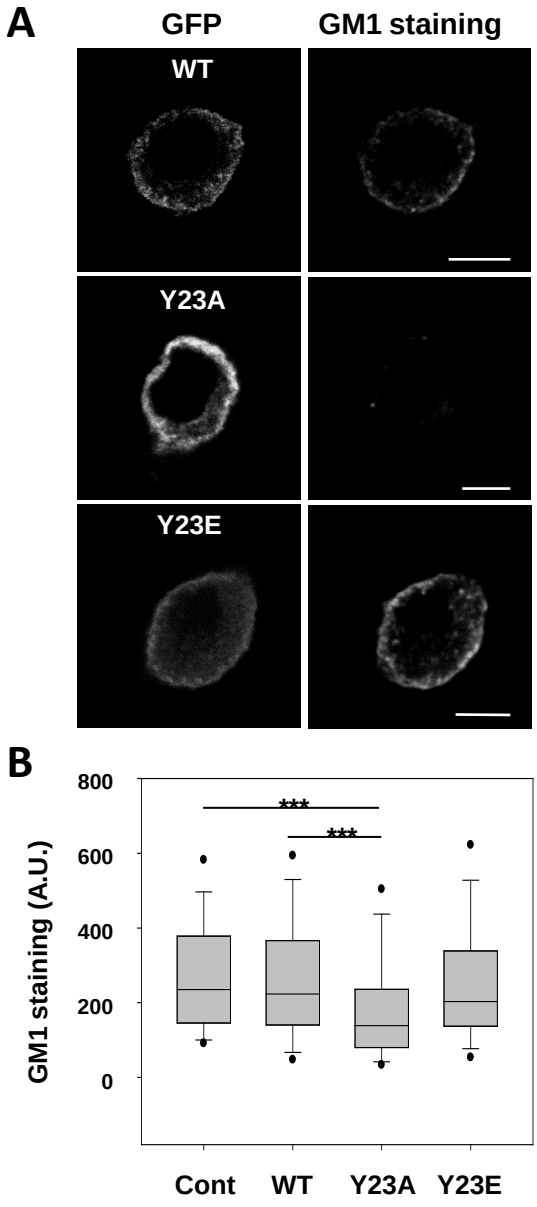

Figure 3: Tyr23 phosphorylation of AnxA2 is required for lipid domain formation

A. Cells expressing AnxA2 WT-GFP, AnxA2 Y23A-GFP or AnxA2 Y23E-GFP were stimulated with 59 mM K^+ in the presence of fluorescent cholera toxin to visualize GM1-enriched domains. Confocal images were recorded in the same optical section. Bars = 5µm.

B. Semi-quantitative analysis of cholera toxin (GM1) labeling in stimulated cells expressed in arbitrary units (± SEM ; $n \geq 15$). Control condition corresponds to non transfected cells. Statistical significance for medians was determined using a Mann-Whitney test. Asterisks indicate statistical significance (***= $P < 0.001$). The experiment has been done on three different cell cultures.

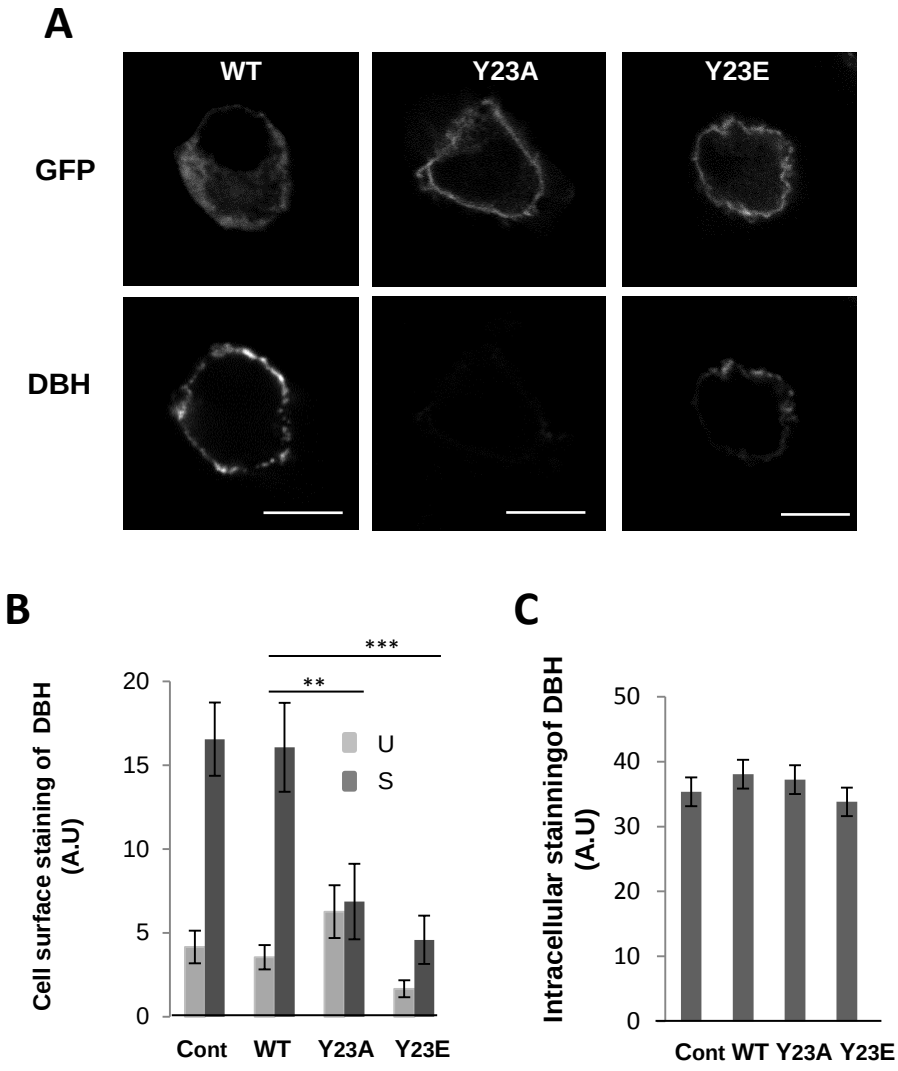

Figure 4 : AnxA2 Tyr23 phosphorylation/dephosphorylation inhibits exocytosis

A. Cells expressing AnxA2-WT-GFP (WT), AnxA2-Y23A-GFP(Y23A) or AnxA2-Y23E-GFP (Y23E) were stimulated with 59 mM K^+ in the presence of DBH antibodies to label exocytotic sites. Cells were then fixed and incubated with secondary antibodies coupled to AlexaFluor-555. Confocal images were recorded in the same optical section. Bars = 5µm.

B. Semi-quantitative analysis of cell surface labeling of DBH in unstimulated (U) and stimulated (S) chromaffin cells expressed in arbitrary units (± SEM ; n ≥12 cells/condition). The control condition corresponds to non transfected cells. Statistical significance for medians was determined using a Mann-Whitney test. Asterisks indicate statistical significance (** p<0,01, *** p<0,001). The experiment has been done on three different cell cultures.

C. Semi-quantitative analysis of intracellular DBH labeling in chromaffin cells. The values were expressed in arbitrary units (± SEM ; n ≥35 cells/condition). The control condition corresponds to non transfected cells. Statistical significance for medians was determined using a Mann-Whitney test, there was not statistically significant difference between the different groups. The experiment has been done on two different cell cultures.

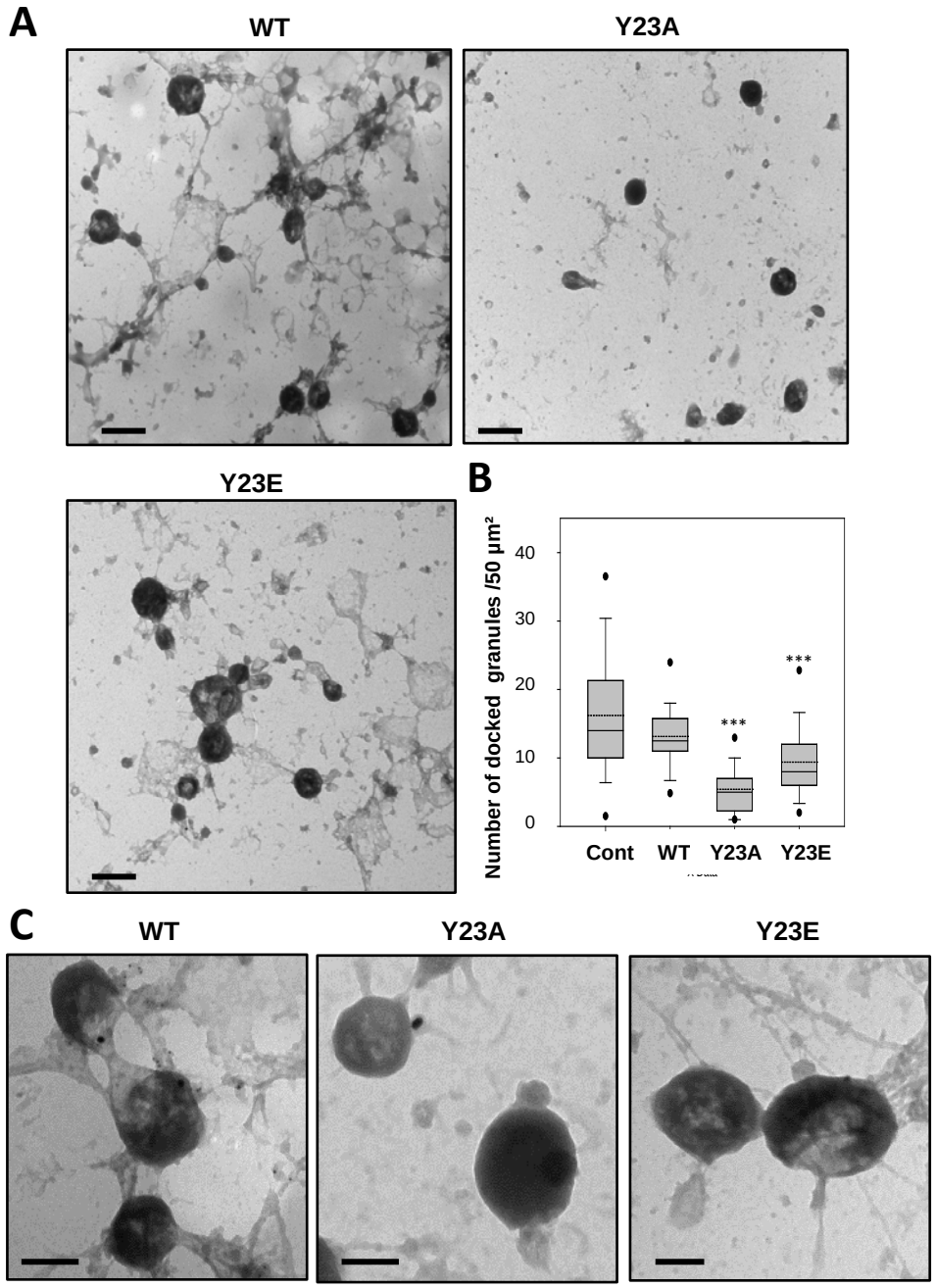

Figure 5 : Phosphorylation state of AnxA2-Tyr23 affects docking of secretory granules.

A. Representative electron micrographs of plasma membrane sheets prepared from stimulated chromaffin cells transfected with AnxA2-WT-GFP (WT), AnxA2-Y23A-GFP (Y23A), or AnxA2-Y23E-GFP (Y23E). Transfected cells were labelled with anti-GFP antibodies and revealed with 25 nm gold particles. Bars = 500nm.

B. Number of granules morphologically docked on plasma membrane sheets prepared from stimulated non transfected cells (Cont) or stimulated cells expressing A2-WT, A2-Y23A, or A2-Y23E (± SEM n $\geq$ 30 images). Asterisks indicate statistical significance for medians (black line) determined using a Mann-Whitney test; the dotted lines represent the means. Images were acquired from three different culture preparations.

C. Representative electron micrographs at higher magnification of plasma membrane sheets prepared from stimulated cells transfected with the indicated AnxA2 constructs. Bars = 100 nm.

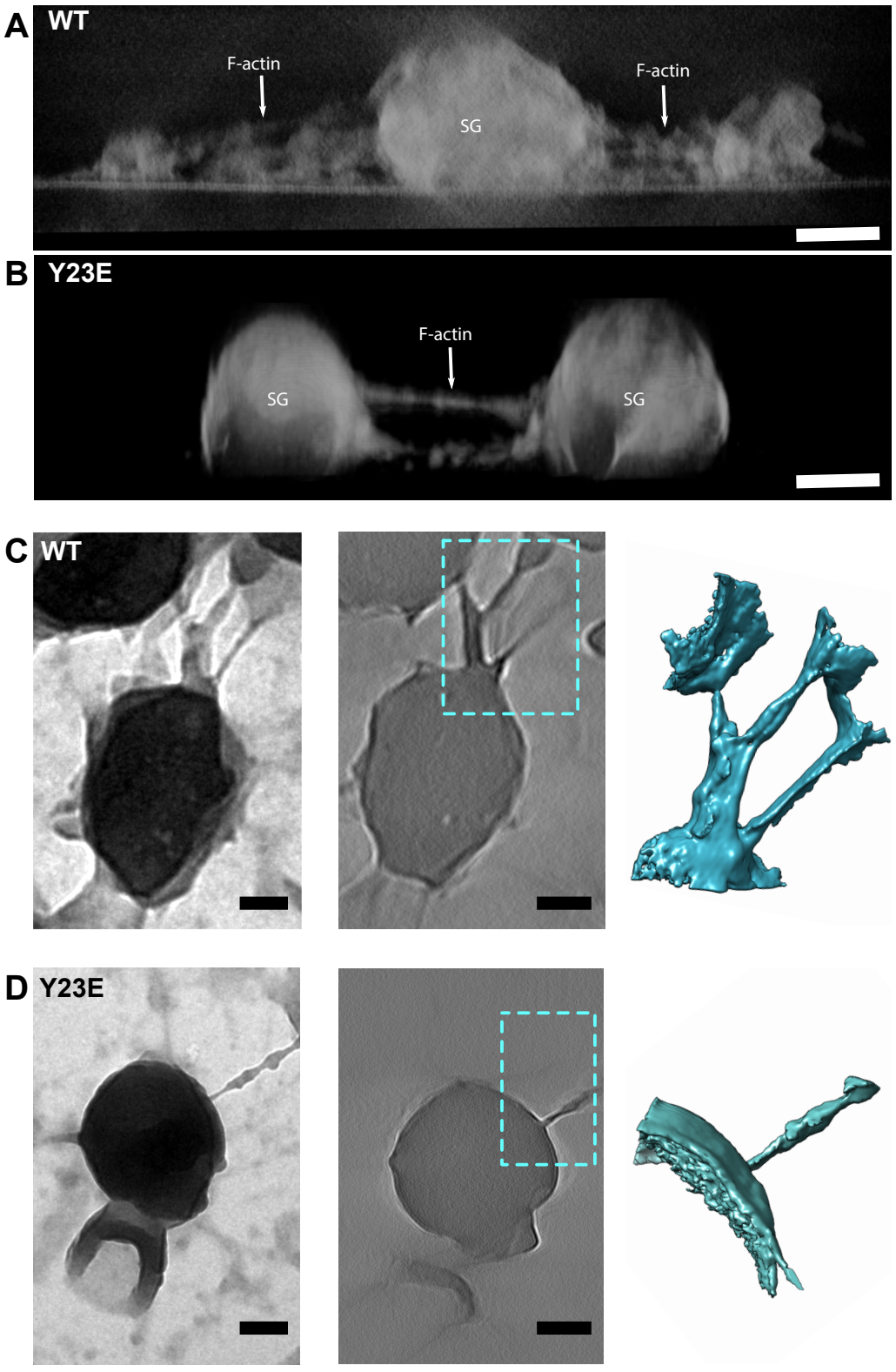

Figure 6 : Phosphorylation of Tyr23 prevents the formation of F-actin bundles essential to anchor secretory granule to the plasma membrane.

All Images were obtained after electron tomography 3D reconstruction of plasma membrane sheets of stimulated cells transfected with AnxA2-WT-GFP (WT) or AnxA2-Y23E-GFP (Y23E).

A. Side view of docked secretory granule (SG) showing F-actin bundles connecting granule to the plasma membrane in A2-WT cells. Bar = 100 nm.

B. Side view of docked secretory granules showing a defect of F-actin bundles formation around granules in the AnxA2-Y23E cells. Bar = 100 nm.

C – D TEM images at zero tilt, tomographic section of docked secretory granules and 3D rendering of F-actin associated to secretory granule in AnxA2-WT and A2-Y23E cells. Bars = 100 nm.

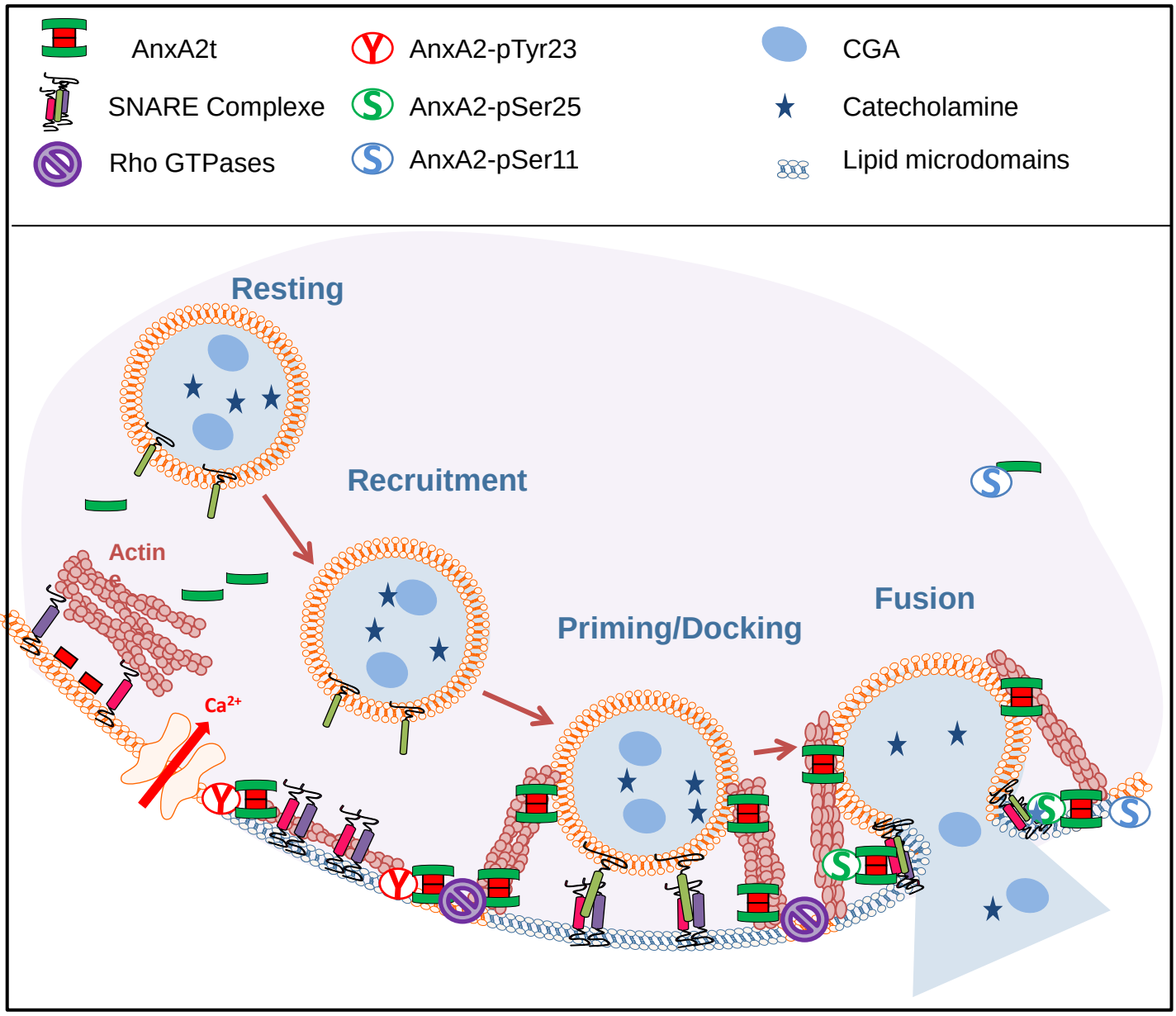

Figure 7 : Multi-functions of AnxA2 during exocytosis : control by Tyr and Ser phosphorylations
Upon cell stimulation, AnxA2 is recruited to the plasma membrane to form a tetramer with the S100A10 protein. At the plasma membrane, AnxA2 phosphorylated on Tyr23 stabilizes lipid micro-domains required to recruit/organize the priming/docking machinery. Tyr23 dephosphorylation is then needed to promote the formation of actin bundles that strongly anchor secretory granules to the exocytotic sites and to allow Ser25 phosphorylation necessary to secretory granule fusion. During this step, AnxA2 and actin bundles regulate the fusion pore opening and participate in the expulsion of the granular content. Finally, phosphorylation of AnxA2-Ser 11 leads to the dissociation of the heterotetramer and the release of the AnxA2 monomer in cytoplasm.

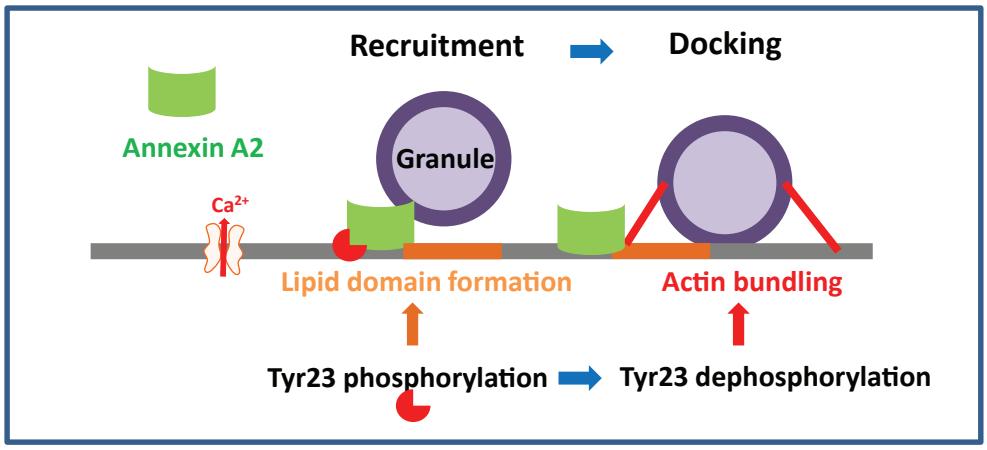
Recruitment
Docking
Annexin A2
Granule
Ca2+
Lipid domain formation
Actin bundling
Tyr23 phosphorylation
Tyr23 dephosphorylation